Adsorption 2, 69–76 (1996)

Structural Transitions at Solid-Liquid Interfaces

RAVI K. BALLAMUDI AND IOANNIS A. BITSANIS*
Department of Chemical Engineering, University of Florida, Gainesville, FL 32611

Received January 6, 1995; Revised March 27, 1995

Abstract. In this paper we present the findings of our investigations using molecular dynamics, on molecularly thin films of *n*-octane confined between topographically smooth solid surfaces. We focus on the effect of increasing solid surface-methylene unit energetic affinity and the effect of increasing pressure (normal load) of the film in inducing liquid-solid phase transitions. We observed an abrupt transition in the structural features of the film at a critical value of the characteristic energy that quantified the affinity between solid surfaces and methylene units. This energetically driven transition was evident from the discontinuous increase of intermolecular order, a precipitous extension of the octane molecules and freezing of molecular migration and rotation. Increasing pressure had a similar effect in inducing a liquid-solid phase transition. The characteristics of the transition showed that it is a mild first order transition from a highly ordered liquid to a poorly organized solid. These findings demonstrate that the solidification of nanoscopically thin films of linear alkanes is a general phenomenon (driven either energetically or by increasing pressure), and does not require the aid of commensurate surface topography.

Keywords: ultra thin films, molecular dynamics, *n*-alkanes and phase transitions

1. Introduction

The structural features and the rheological properties of nanoscopically thin films of short alkanes and other oligomeric lubricants can be drastically different from those of the corresponding bulk liquids. Understanding the microscopic origin of confinement induced changes is essential for rational material selection and efficient process design in diverse phenomena as nanotribology, polymer extrusion ("melt fracture"), wetting and spreading of liquids, flow through microporous media, flocculation of colloids and heterogeneous catalysis (Homola et al., 1990; Denn, 1990).

Experimental advances in the past decade have made the study of molecularly thin films possible. Several shear flow experiments using Surface Force Apparatus (SFA) (Israelachvili and Adams, 1978; Israelachvili et al., 1988; Van Alsten and Granick, 1988) have reported that films consisting of fewer than 4-5 segmental, or molecular layers would not flow until a critical 'yield' stress was applied (Homola et al., 1991; Granick, 1991). Squeezing flow SFA experiments reported a stepwise response similar to the peeling of discrete layers (Chan and Horn, 1985). Squeezing flow experiments on very dense micellar solutions resulted in similar findings (Nikolov and Wasan, 1989; Nikolov et al., 1990). Scanning Tunneling Microscopy experiments detected highly ordered domains (microcrystallites) in monolayers of oligomers deposited on metal surfaces (Rabe and Buchholz, 1991; Hentske et al., 1992).

The microscopic origin of these phenomena was probed by numerous molecular simulations. The first simulation studies (Magda et al., 1985; Bitsanis et al., 1987; 1990) were consistent with a "liquid-like" pattern of interfacial and thin film behavior. Subsequent studies stressed the importance of solid surface topography (Schoen et al., 1988) and revealed the possibility of "epitaxial" crystallization, i.e., the development of solid-like features inside the layer immediately adjacent to the solid surface (Thompson and Robbins, 1990).

*Author to whom correspondence should be addressed.

Koopman et al. (1994), reported the formation of highly ordered *micro-domains* inside the layers immediately adjacent to the solid surfaces. The domains possessed the order of "rotator" hydrocarbon phases, were stable on the nsec timescale and their directionality was imposed by the underlying square solid matrix.

The combined findings of experiments and computer "experiments" have revealed a rich and diverse behavior of interfacial and confined "liquid" films. In some cases the behavior could be classified as "liquid-like" with only moderate differences from the bulk. Other simulations and experiments suggested "glassy" features. Finally, several experiments and simulations observed the development of solid-like features.

The many factors that affect the properties of interfacial and thin films can be classified in four categories:

a) thermodynamic conditions (temperature and pressure)
b) energetics of the solid-liquid interaction
c) topography of the underlying solid substrate
d) architecture of the liquid molecules

Clearly, the behavior of the film is determined by a complex interplay among all these factors. Any attempt to "tailor" thin films with the desired type of behavior requires at least a qualitative understanding of the relative importance of each factor. The objective of this paper is to contribute towards reaching such a level of understanding. Our approach consists in isolating one among the above factors and studying its effect on the film's properties. Factors a) and b) (thermodynamic conditions and energetics) are easily quantifiable. Furthermore, there exists evidence that they are more important than factors related to surface topography. This seems to be a logical conclusion of the fact that solid-like thin film behavior was observed for a variety of liquids whose molecules were not particularly commensurate with the underlying solid substrate (cleavage plane of mica).

In order to accomplish our objective we opted to simulate thin films of n-octane confined between atomically smooth 10-4 Lennard-Jones surfaces under conditions of constant pressure and constant temperature. The choice of n-octane offers several advantages, since extensive data on bulk n-octane and wider films of the same liquid are available from previous simulation studies (Gupta et al., 1994; Koopman et al., 1994). Furthermore, several experiments investigated films of short linear alkanes (Homola et al., 1991; Granick, 1991; Israelachvili et al., 1988; Chan and Horn, 1985).

The rest of this paper has been organized as follows: Section 2 describes the simulation method, conditions and molecular models employed. Section 3 presents our findings and Section 4 examines their implications. Finally, Section 5 provides a brief summary of the most important results reported in this paper.

2. Molecular Model and Simulation Method

In all simulations the octane films were confined between two parallel, geometrically flat solid planes. The segment density normal to the solid surfaces always exhibited the normal oscillatory behavior (Koopman et al., 1994).

To study of the effect of solid-methylene unit energetic affinity the simulations were conducted on films with the following features. The distance between the solid walls is determined by the following two requirements: a) Formation of three distinct methylene unit layers. b) The attainment of a desired value of pressure normal to the solid surface. Furthermore, the temperature was kept close to its prespecified value by velocity scaling every 50 time steps (Andrea et al., 1983). Therefore, our simulations were performed in a constant N, V, T (canonical) ensemble. A fixed film thickness was chosen to yield a selected value of the (normal) pressure and a fixed specific volume. This implies that the films were at thermodynamic equilibrium with a bulk reservoir at the same temperature and a bulk pressure equal to the normal component of the pressure tensor inside the film. Hence, film and the bulk reservoir have the same chemical potential.

The effect of pressure was studied by fixing the solid-methylene unit energetic affinity to a constant value. The distance between the solid walls is adjusted to yield different specific volumes resulting in a range of pressures. Each simulation was performed at a constant average normal pressure.

The model of the octane chain uses the "United Atom" approach, which treats CH_2 and CH_3 groups as identical spherically symmetric units. The integrity of the molecules was maintained using the following potentials: a) a harmonic bond length potential b) a harmonic bond angle potential c) a torsional potential (Koopman et al., 1994; Ryckaert and Bellamans, 1978).

The interactions between segments of different chains as well as segments of the same chain separated by more than three bonds were of the 12-6 Lennard-Jones type. The value of the inter-segment Lennard-

Jones parameter for methyl and methylene units was 60.1 K. The segment-solid wall interactions were modeled by a 10-4 Lennard-Jones potential

$$U_{sl}(z/\sigma_{sl}) = 2\pi\rho_s\varepsilon_{sl}\{0.4(z/\sigma_{sl})^{-10} - (z/\sigma_{sl})^{-4}\} \quad (1)$$

In the above equation z is the surface-segment distance, ρ_s is the number density of the solid layer, ε_{sl} is the Lennard-Jones energy parameter for the interaction between segments and a (fictitious) surface atom and σ_{sl} is the arithmetic average of the Lennard-Jones length parameters for segments and surface "atoms" and segments over an entire solid layer. After the smearing of solid atoms the resulting surface becomes perfectly smooth and lacks any topographical features. Since, for such a surface only the product $\rho_s\varepsilon_{sl}$ and not the individual factors are meaningful, ρ_s was arbitrarily assigned the value 1.0 in molecular dynamics units.

In this paper we discuss the results of the simulations performed at the following conditions: a) the temperature 300.5 K and the (normal) pressure close to 0 bar for the following values of the solid-segment energy parameter ε_{sl}: 180.3 K, 240.4 K, 300.5 K, 360.6 K, 420.7 K and 480.8 K. b) the temperature 360.6 K and the solid-segment energy parameter (ε_{sl}) 601 K for the following values of normal pressure on the film: 1090, 710, 1320, 980, 490, 150, −40 bar.

Bulk octane is a liquid in all the simulations. The freezing point and boiling point of n-octane are 216.4 K and 398.8 K at normal conditions (1 bar pressure). Estimates using the Clausius-Claperon equation showed that increasing the pressure on bulk n-octane to 1500 bar elevates its melting point by only 10 to 20 K. Clearly, bulk n-octane is a liquid for all the pressures studied.

3. Results

In this section we discuss the effect of increasing solid-segment affinity ε_{sl} and increasing pressure P, in inducing structural transitions in thin films. Since both ε_{sl} and P induce qualitatively similar features in the films, we discuss their effect simultaneously.

Figure 1 contains the average film density as a function of ε_{sl}. The overall shape of the curve in Fig. 1 is similar to typical high adsorption isotherms with a noticeably abrupt densification of the film between the ε_{sl} values 300.5 K and 360.6 K. Figure 2 shows the normal component of pressure tensor as a function of specific volume. The shape of the curve in Fig. 2 is typical of

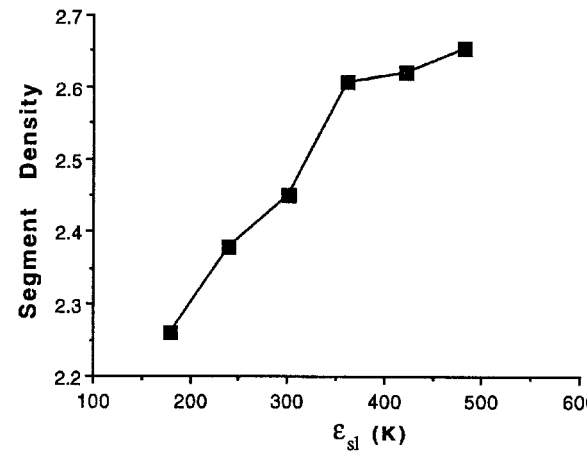

Figure 1. Average film density (segments per unit volume) as a function of ε_{sl}.

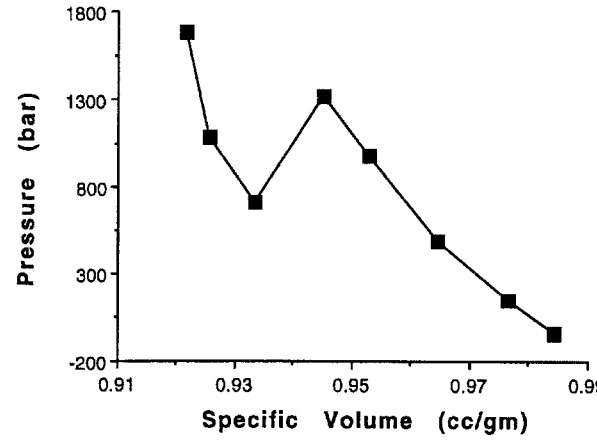

Figure 2. Pressure (in bar) as a function of specific volume (cc/gm).

PV isotherms involving phase transitions. Metastable states can be observed as a result of the finite duration of the simulations (a 3-4 nsec). This is a well known phenomenon in canonical ensemble simulations (Allen and Tildesley, 1989; Alder and Wainwright, 1962; Mayer and Wood, 1965). The specific volume of the film is much lower than that of bulk n-octane (1.4235 cc/gm at 298 K and 1 bar), which is to be expected since it is confined between highly adsorbing surfaces.

The in-layer pair correlation function (PCF) offers good insight into the structural properties of the film layers. Figures 3a and 3b show the first and middle layer PCF's for various ε_{sl} values. Figures 4a and 4b show the PCF's for several values of the pressure (P). The initial part of the pair correlation function which mostly reflects trivial intrachain correlations, has been omitted. An immediately apparent feature is that

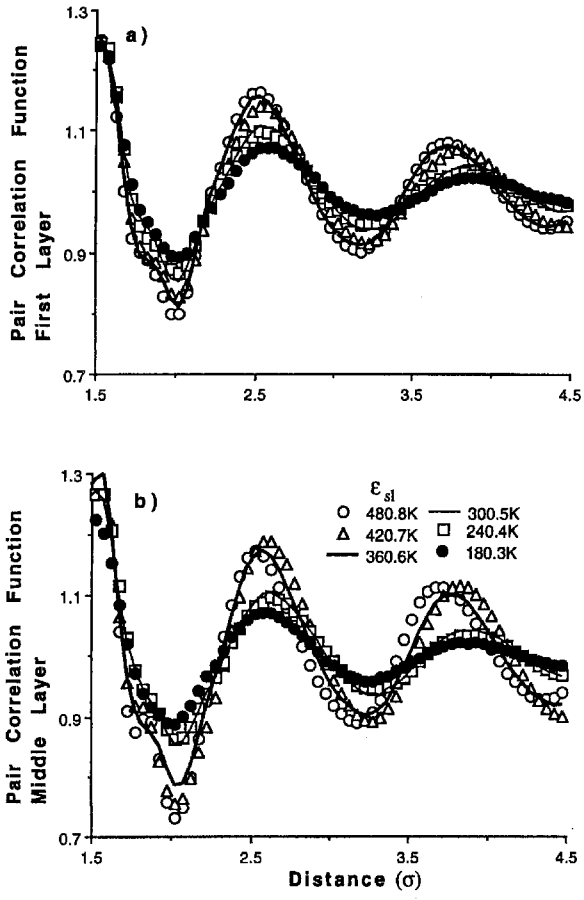

Figure 3. Pair correlation function of the octane molecules at $T = 300.5$ K for several values of ε_{sl}. a) First layer, b) middle layer. We see a discontinuous transition between $\varepsilon_{sl} = 300.5$ K and $\varepsilon_{sl} = 360.6$ K.

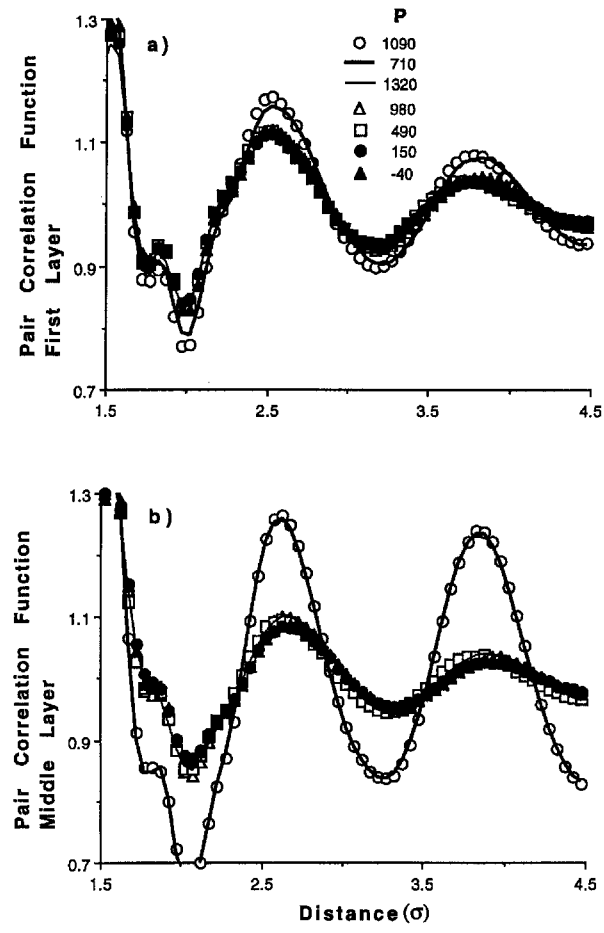

Figure 4. Pair correlation function of the octane molecules for several values of pressure. a) First layer, b) middle layer. Similar behavior observed in Fig. 3 can be seen between $P = 710$ bar and $P = 1320$ bar.

the PCF curves belong to one of two distinct groups. In Fig. 3 the shape of the PCF undergoes an abrupt change at some critical ε_{sl} value (between 300.5 K and 360.6 K). A similar change is evident at a critical value of P in Fig. 4 (between 1320 and 710). Such abrupt changes in the shape of the PCF are characteristic of first order phase transitions. One of our simulations resulted in a thermodynamic state which is genuinely unstable, i.e., with a negative isothermal compressibility. This point is not shown in Fig. 2. This state was characterized by the co-existence of more than one phase at values of specific volume between 0.9451 and 0.9334. Such behavior is manifested by different inlayer PCF curves for the two layers immediately adjacent to the two solid surfaces. These PCF curves for surface layers belong to separate groups of curves evident in Fig. 4, i.e., one of these layers exhibits solid-like structure and the other liquid-like structure.

The fraction of trans angles showed a discontinuous jump corresponding to the precipitous change in the shape of the PCF curve. Figures 5a and 5b depict the percentage trans angles as a function of ε_{sl} and P respectively. Between the ε_{sl} values of 300.5 K and 360.6 K the fraction of trans angles sharply raises from 0.83 to 0.90. A similar sharp increase in the percent of trans angles occurs as P crosses its critical value between 710 bar and 1320 bar.

The discontinuous structural changes are accompanied by the freezing of molecular migration and rotation. The mean square displacement (MSD) and the time correlation function of the molecular end-to-end vector (rotational correlation function, RCF) are good measures of molecular mobility. The slope of the former is proportional to the translational self-diffusion

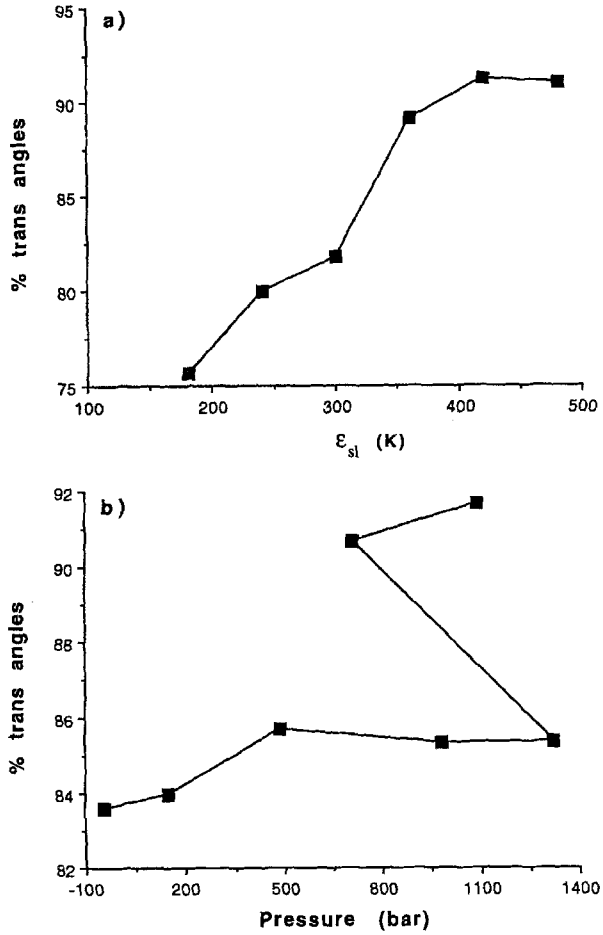

Figure 5. The percentage of trans angles as a function of the parameter a) ε_{sl}, a sharp increase in the number of trans angles is evident between $\varepsilon_{sl} = 300.5$ K and $\varepsilon_{sl} = 360.6$ K. b) P, a similar increase can be seen between $P = 710$ bar and $P = 1320$ bar.

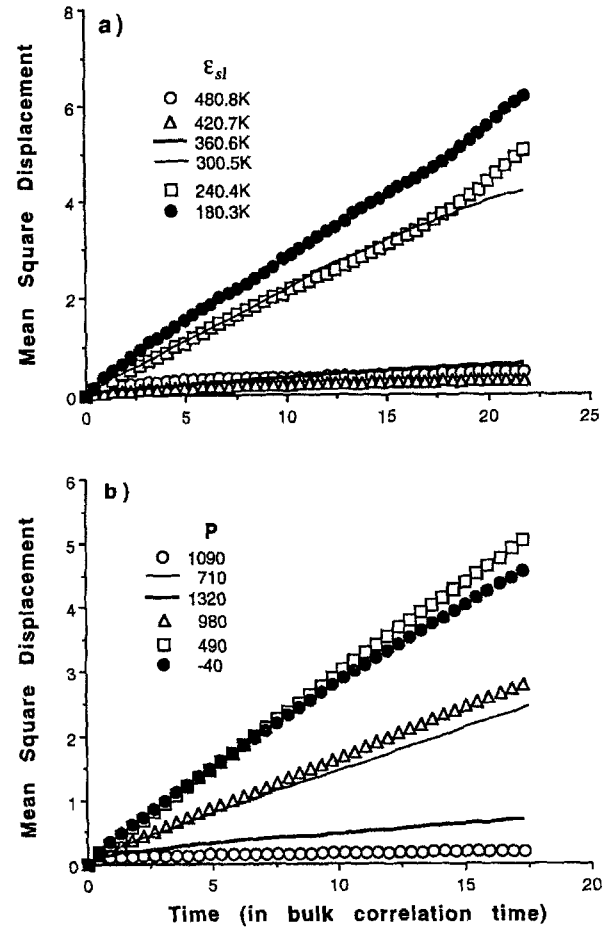

Figure 6. Chain center of mass mean square displacement parallel to the surface, in the surface layer. The ordinate has been scaled by the radius of gyration (in one direction) of bulk octane. The curves for the higher ε_{sl} and for pressures beyond the transition pressure are very close to the abscissa, indicating a solid like behavior. The sharp change in the displacement is evident in both the cases.

coefficient, while that of the latter is proportional to the rotational diffusivity.

Figures 6a and 6b contain the MSD curves of the octane chains over a period of 0.2 nsec for several ε_{sl} and P values. These MSD curves represent intralayer motions, i.e., segmental displacements in the two directions parallel to the solid surfaces. Above the critical ε_{sl} value the MSD of the chain centers of mass was much smaller than the molecular dimensions. Similarly above the critical P value the molecular migration is negligible. Also any significant molecular rotation stops at the same values of solid-segment affinity and pressure (see Figs. 7a and 7b).

The cleavage plane of mica used in most SFA experiments is a strongly adhesive surface. Estimates of its effective ε_{sl} range from 360 K to 600 K, which places it well above the transition threshold at room temperature. This conclusion is further reinforced by the fact that the surface density of mica (ρ_s) has value considerably higher than 1.0 in our units (see Eq. 1 and the discussion following it). Though the effect of pressure could have been investigated at a lower temperature, we chose to simulate a system at a temperature considerably over the room temperature (360.6 K). The effect of pressure in inducing structural transitions even at such an elevated temperature emphasizes the critical role normal forces play in the research of thin film characteristics using SFA. Therefore, confinement lead to a pressure-driven solidification at pressures much lower than those required for similar solidification of bulk n-octane at $T = 360$ K.

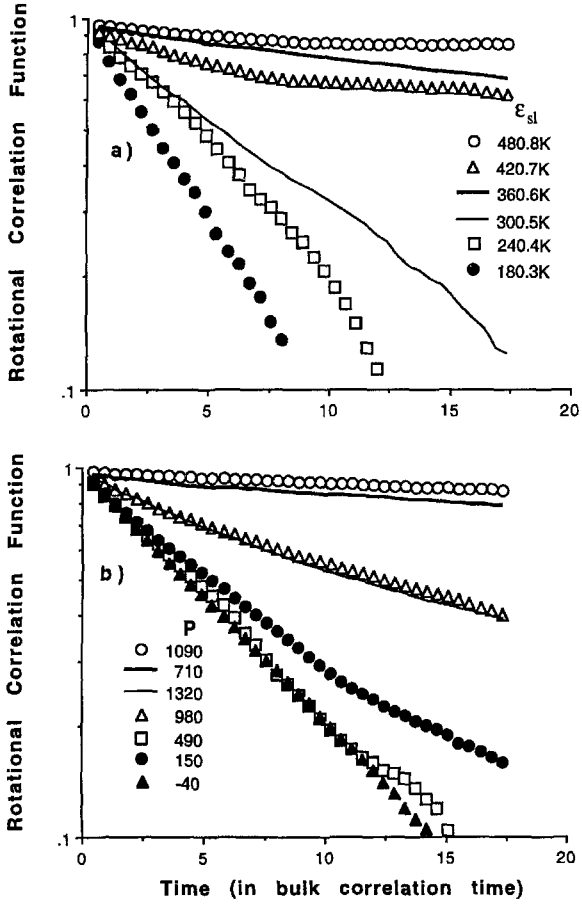

Figure 7. The rotational correlation function of the octane chains in the film illustrating the freezing of rotational motion of the chains beyond the transition. a) ε_{sl}, b) P.

4. Discussion

In this section we discuss further our findings and examine some of their implications. We also comment on the relation between the simulated systems and actual thin films studied experimentally.

We start with a close examination of the ordered phases above the critical ε_{sl} and P. Figure 8 contains typical snapshots of first layer configurations at four different ε_{sl} values: ε_{sl} = 180.3 K, 300.5 K, 300.6 K, 480.8 K at the temperature of 300.5 K. Figure 9 contains similar first layer snapshots at the following P values: $P = -40$, 1320, 710, 1090 bar.

One prominent characteristic of the most ordered configurations (Figs. 8d and 9d) is the presence of two distinct domains with their directors approximately normal to each other. The formation of two such domains is apparent in many such ordered phases.

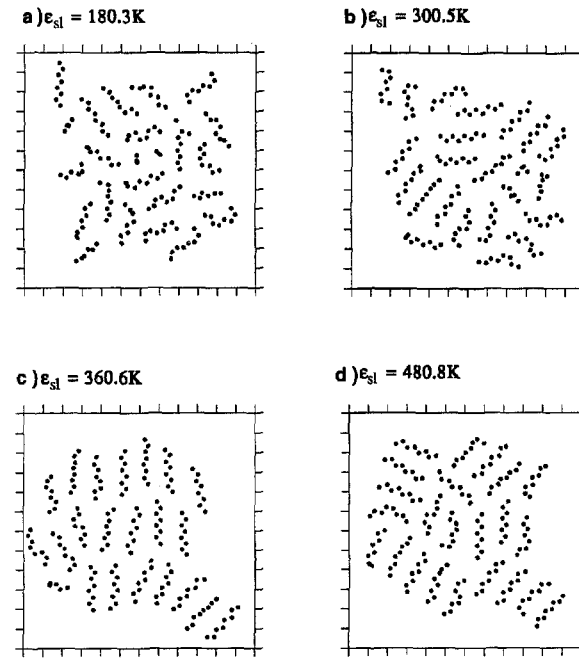

Figure 8. "Snapshots" (projection on the plane parallel to surface) of first layer octane chains for several values of ε_{sl}. The distance between ticks on axes represents one methylene unit diameter. Some chains seem to have fewer than 8 segments because they are not fully in the first layer. We see a sudden ordering of the chains between ε_{sl} = 300.5 K and ε_{sl} = 360.6 K and formation of stable micro-domains.

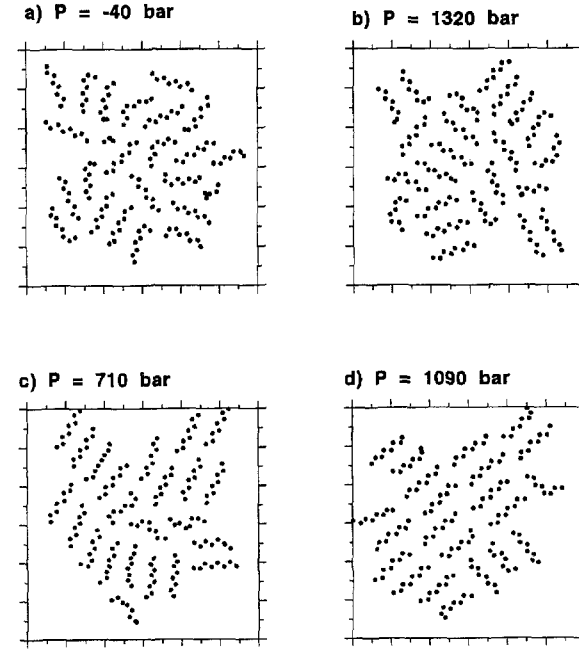

Figure 9. Same as Fig. 8, but for several values of pressure. We see the formation of ordered domains beyond the transition point (P = 1320 bar).

The domains were stable over the time scale of the simulations (1-2 nsec). The presence of the ordered domains instead of a uniform ordered phases lead to the formation of two "grains" through out the whole film. Each grain typically contained about 20–50 octane molecules. Simulations of smaller systems with periodic dimensions 6σ (2.4 nm) always led to the formation of a uniform ordered phase. Therefore, we can conclude that the linear dimensions of these domains should be intermediate between 2 to 3 nm. This is close to the domain size inferred from Scanning Tunneling Microscopy experiments of oligomer monolayers deposited on metal surfaces (Rabe and Bucholz, 1991; Hentske et al., 1992). However, it is possible that the domains are frozen metastabilities that cannot relax on the time scale of the simulations.

Above the transition values of ε_{sl} and P the film can be characterized as a solid. The presence of orientational order and considerable translational order perpendicular to the molecular end to end vector are characteristic of a 2-dimensional smectic. However, no order in the direction parallel to the chain end to end vector can be observed (Figs. 8c,d, 9c,d). So we can safely chatacterize the film as a solid (at least a granular solid), very similar to the "rotator" phases of bulk alkanes. Nevertheless, it is a poorly organized solid (Figs. 8c, 9c) as manifested by the presence of a few large defects (i.e., presence of partial chains) and numerous small defects (i.e., gauche sequences of ordered chains).

Immediately below the transition threshold of ε_{sl} and above the transition value of P the film is clearly a liquid. This can be readily inferred from the high degree of molecular diffusion and rotation (Figs. 6 and 7). However, it is a considerably more "viscous" and considerably more "ordered" liquid than bulk octane. Figures 8b and 9b illustrate the presence of strong intermolecular order just below the transitions ($\varepsilon_{sl} = 300.5$ K, $P = 1320$ bar).

5. Summary

We have presented the results of two sets of molecular dynamics simulation studies designed to explore the effect of increasing solid-segment affinity and increasing normal pressure in molecularly thin n-octane films. The solid surfaces were devoid of any topographical features and were modeled as atomically smooth 10-4 Lennard-Jones planes.

In both simulations we observed a sharp transition in the structural features of the film at some critical value of ε_{sl} and P. The transition is signaled by a discontinuous change in the intermolecular order and is facilitated by a sharp extension of the n-octane molecules. The transition is a first order phase transition from a strongly ordered liquid to a weakly organized solid. The molecules formed stable micro-domains over the timescale of the simulation ($\sim$2 nsec).

These findings demonstrate that the solidification of nanoscopically thin films of linear alkanes under the conditions where bulk octane is a liquid is a generic, energetically driven phenomenon. Pressure has a similar effect on solidifying the thin films. The solidification does not require the aid of commensurate surface topography of the underlying solid substrate, though it may be promoted or suppressed by the topography of the confining surfaces.

Our simulations provide a natural explanation to the solid like features reported in several experimental studies of thin linear alkane films. Furthermore, they show that the cleavage plane of mica, which is the most commonly used confining surface in these experiments, is certainly adhesive enough to induce solidification of the confined film and can do so without being topographically commensurate with the molecules of the confined film.

Nomenclature

ε_{sl}	energy parameter between solid surface and methylene segment
P	normal component of pressure on the film boundaries
U_{sl}	potential energy function for the solid-methylene segement interactions
z	perpendicular distance between the segment and solid surface
ρ_s	segment density of the surface
σ_{sl}	length parameter for solid-segment interactions

Acknowledgments

The authors would like to acknowledge the financial support of the Engineering Research Center (ERC) for Particle Science and Technology at the University of Florida, the National Science Foundation (NSF) grant number: EEC-94-02989, and the Industrial Partners of the ERC.

References

Alder, B.J. and T.E. Wainwright, *Phys. Rev.*, **127**, 359 (1962).

Allen, M.P. and D.J. Tildesley, *Computer Simulation of Liquids*, p. 292, Oxford Publ., 1989.

van Alsten, J. and S. Granick, *Phys. Rev. Lett.*, **61**, 2570 (1988).

Andrea, T.A., W.C. Swope, and H.C. Anderson, *J. Chem. Phys.*, **79**, 4576 (1983).

Bitsanis, I., J.J. Magda, M. Tirrell, and H.T. Davis, *J. Chem. Phys.*, **87**, 1733 (1987).

Bitsanis, I., S.A. Somers, H.T. Davis, and M. Tirrell, *J. Chem. Phys.*, **93**, 3427 (1990).

Bitsanis, I.A. and C. Pan, *J. Chem. Phys.*, **99**, 5520 (1993).

Chan, D.Y. and R.G. Horn, *J. Chem. Phys.*, **83**, 5311 (1985).

Denn, M.M., *Ann. Rev. Fluid Mech.*, **22**, 13 (1990).

Edberg, R., D.J. Evans, and R.J. Moriss, *J. Chem. Phys.*, **84**, 6933 (1986).

Fixmann, M., *J. Chem. Phys.*, **69**, 1527 (1978).

Granick, S., *Science*, **253**, 1374 (1991).

Gupta, S., D.C. Koopman, G.B. Westermann-Clark, and I.A. Bitsanis, *J. Chem. Phys.*, **100**, 8444 (1994).

Gupta, S., G.B. Westermann-Clark, and I. Bitsanis, *J. Chem. Phys.*, **98**, 634 (1993).

Hamza, A.V. and R.J. Madix, *Surf. Sci.*, **179**, 25 (1987).

Hentske, R., B.L. Schurmann, and J.P. Rabe, *J. Chem. Phys.*, **92**, 6213 (1992).

Homola, A.M., H.V. Nguyen, and G. Hadziioannou, *J. Chem. Phys.*, **94**, 2346 (1991).

Homola, A.M., G.B. Street, and C.M. Mate, *MRS Bulletin*, **XV**(3), 45 (1990).

Israelachvili, J.N., and D. Tabor, *Proc. R. Soc. London Ser. A*, **331**, 19 (1972).

Israelachvili, J.N. and G.E. Adams, *J. Chem. Soc. Faraday Trans.*, **174**, 975 (1978).

Israelachvili, J.N., P.M. McGuiggan, and A.M. Homola, *Science*, **240**, 189 (1988).

van Kampen, N.G., *Stochastic Processes in Physics and Chemistry*, North Holland Publ., 1981.

van Kampen, N.G., *Appl. Sci. Res.*, **37**, 67 (1981).

Koopman, D.C., S. Gupta, R.K. Ballamudi, G.B. Westermann-Clark, and I.A. Bitsanis, *Chem. Eng. Sci*, **49**, 2907 (1994).

Knudstrup, T.K., I.A. Bitsanis, and G.B. Westermann-Clark, *Langmuir* (1994) (accepted).

Magda, J.J., M. Tirrell, and H.T. Davis, *J. Chem. Phys.*, **83**, 1888 (1985).

Mayer, J.E. and W.W. Wood, *J. Chem. Phys.*, **42**, 4268 (1965).

Mongomery Jr., J.A., S.L. Holmgren, and D. Chandler, *J. Chem. Phys.*, **73**, 3688 (1980).

Nicholson, D. and N.G. Parsonage, *Computer Simulation and the Statistical Mechanics of Adsorption*, Academic Press, 1982.

Nikolov, A.D. and D.T. Wasan, *J. Coll. Inter. Sci.*, **133**, 1 (1989); **133**, 13 (1989).

Nikolov, A.D., D.T. Wasan, N.D. Denkov, P.A. Kralchesvky, and I.B. Ivanov, *Prog. Coll. Pol. Sci.*, **82**, 1 (1990).

Padilla, P. and S. Toxvaerd, *J. Chem. Phys.*, **94**, 5650 (1991).

Peanasky, J., L.L. Cai, and S. Granick, *Macromolecules* 1994 (in print).

Rabe, J.P. and S. Buchholz, *Phys. Rev. Lett.*, **66**, 2096 (1991).

Rigby, D. and R.J. Roe, *J. Chem. Phys.*, **87**, 7285 (1987).

Ryckaert, J.P. and A. Bellemans, *Faraday Discuss. Chem. Soc.*, **66**, 95 (1978).

Ryckaert, J.P., G. Ciccotti, and H.L.C. Berendsen, *J. Comput. Phys.*, **23**, 327 (1977).

Schoen, M., J.H. Cushman, D.J. Diestler, and C.L. Rhykerd Jr., *J. Chem. Phys.*, **88**, 1394 (1988).

Tabor D. and R.H.S. Winterton, *Proc. R. Soc. London Ser. A*, **312**, 543 (1969).

Thompson, P.A. and M.O. Robbins, *Phys. Rev. A*, **41**, 6830 (1990).

Thompson, P.A., G.S. Grest, and M.O. Robbins, *Phys. Rev. Lett.*, **68**, 3448 (1992).

Toxvaerd, S.J., *J. Chem. Phy.*, **93**, 4290 (1990).

Weber, T.A., *J. Chem. Phys.*, **69**, 2347 (1978); **70**, 4277 (1979).

Xia, T.K., J. Quyang, M.W. Ribarsky, and U. Landman, *Phys. Rev. Lett.*, **69**, 1967 (1992).